Concentration, sources and light absorption characteristics of dissolved organic carbon on a typical glacier, the northern Tibetan Plateau

F. Yan[1,4,5], S. Kang[1,3], C. Li[2,3], Y. Zhang[1], X. Qin[1], Y. Li[2,4], X. Zhang[1,4], Z. Hu[1,4], P. Chen[2], X. Li[1], B. Qu[5], M. Sillanpää[5,6]

[1]Qilian Station for Glaciology and Ecological Environment, State Key Laboratory of Cryospheric Sciences, Cold and Arid Regions Environmental and Engineering Research Institute, Chinese Academy of Sciences, Lanzhou 730000, China

[2]Key Laboratory of Tibetan Environment Changes and Land Surface Processes, Institute of Tibetan Plateau Research, Chinese Academy of Sciences, Beijing 100101, China

[3]CAS Center for Excellence in Tibetan Plateau Earth Sciences, Chinese Academy of Sciences, Beijing 100101, China

[4]University of Chinese Academy of Sciences, Beijing 100049, China

[5]Laboratory of Green Chemistry, Lappeenranta University of Technology, Mikkeli, Sammonkatu 12, FIN-50130, Finland

[6]Department of Civil and Environmental Engineering, Florida International University, Miami, FL 33174, USA

Correspondence to: C. Li (lichaoliu@itpcas.ac.cn)

Abstract. Light-absorbing dissolved organic carbon (DOC) constitutes a major part of the organic carbon in glacierized regions. It has important influences on the carbon cycle and radiative forcing of glaciers. However, currently, few data are available in the glacierized regions of the Tibetan Plateau (TP). In this study, DOC characteristics of a typical glacier (Laohugou glacier No. 12 (LHG glacier)) in the northern TP were investigated. Generally, DOC concentrations on LHG glacier were comparable to those in other regions around the world. DOC concentrations in snowpits and surface snow were 332 ± 132 μg L^{-1} and 229 ± 104 μg L^{-1}, respectively, which were slightly higher than those of the Greenland ice sheet. DOC concentration of surface ice (superimposed ice) was 426 ± 270 μg L^{-1}, comparable to that of the Antarctic ice sheet. The average discharge-weighted DOC of proglacial streamwater was 238 ± 96 μg L^{-1}, which is lower than that of Mendenhall glacier, Alaska. The annual DOC flux released

from this glacier was estimated to be 6,949 kg C yr^{-1}, of which 46.2 % of DOC was bioavailable and could be decomposed into CO_2 within one month of its release. The mass absorption cross section (MAC) of DOC at 365 nm was 1.4 $\pm$0.4 $m^2 g^{-1}$ in snow and 1.3 $\pm$0.7 $m^2 g^{-1}$ in ice, similar to the values of dust transported from adjacent deserts. Based on this finding and the significant relationship between DOC and Ca^{2+}, the main source of DOC might be desert mineral dust. Meanwhile, autotrophic or heterotrophic biological activities and autochthonous carbon could also contribute to glacier DOC. The radiative forcing of snowpit DOC was considered to be 0.43 W m^{-2}, implying the necessity of accounting DOC of snow for accelerating melt of glaciers on the TP.

Key words: dissolved organic carbon, light absorption, LHG glacier, the Tibetan Plateau

1 Introduction

Ice sheets and mountain glaciers cover 11 % of the land surface of the Earth and store approximately 6 Pg (1 Pg = 10^{15} g) of organic carbon, the majority of which (77 %) is in the form of dissolved organic carbon (DOC) (Hood et al., 2015). The annual global DOC release through glacial runoff is approximately 1.04 ± 0.18 Tg C (1 Tg = 10^{12} g) (Hood et al., 2015). Therefore, glaciers not only play an important role in the hydrological cycle by contributing to sea-level rise (Rignot et al., 2003; Jacob et al., 2012) but also potentially influence the global carbon cycle (Anesio and Laybourn-Parry, 2012; Hood et al., 2015) in the context of accelerated glacial ice loss rates. In addition, a large portion of glacier-released DOC has proven to be highly bioavailable, influencing the balance of downstream ecosystems (Hood et al., 2009; Singer et al., 2012; Spencer et al., 2014).

Although DOC storage in ice sheets is much larger than that of mountain glaciers, the annual mountain glacier-derived DOC dominates the global DOC release (Hood et al., 2015). Currently, many studies on the concentration, age, composition, storage and release of DOC have been conducted around the world (Hood et al., 2009; Stubbins et al., 2012; May et al., 2013; Bhatia et al., 2013; Lawson et al., 2014; Fellman et al., 2015; Hood et al., 2015). The sources of glacier-derived DOC were found to be diverse (Bhatia et al., 2010; Stubbins et al., 2012; Singer et al., 2012; Spencer et al., 2014), with large variations in concentrations and ages (Hood et al., 2009; Singer et al., 2012; Hood et al., 2015). For example, a study on the Greenland ice sheet showed that the concentration of exported DOC exhibited slight temporal variations during the melting period, with subtly higher values in early May than in late May and July (Bhatia et al., 2013). Additionally, the concentration of total organic carbon in snow across the East Antarctic ice sheets exhibited remarkable spatial variations due to the marine source of organic carbon (Antony et al., 2011). Studies on both radiocarbon isotopic compositions and biodegradable DOC (BDOC) have proposed that ancient organic carbon from glaciers was much easier for microbes to utilize in glacier-fed rivers and oceans, implying that large amounts of this DOC will return to the atmosphere quickly as CO_2 and participate in the global carbon cycle, thereby producing a positive feedback in the global warming process (Hood et al., 2009; Singer et al., 2012; Spencer et al., 2014). In addition to black carbon (BC), another DOC fraction known as water-soluble brown carbon has also been considered a warming component in the climate system (Andreae and Gelencsér, 2006; Chen and Bond, 2010). This type of DOC exhibits strong light-absorbing properties in the ultraviolet wavelengths (Andreae and Gelencsér, 2006; Chen and Bond, 2010; Cheng et al., 2011). The relative

radiative forcing caused by water-soluble organic carbon (the same as DOC) relative to BC in aerosols was estimated to account for 2-10 % and approximately 1 % in a typical pollution area of North China (Kirillova et al., 2013) and a remote island in the Indian Ocean (Bosch et al., 2014), respectively. Unfortunately, so far, few direct evaluations have been conducted in the glacierized regions around the world, including the Tibetan Plateau (TP), where DOC accounts for a large part of the carbonaceous matter (Legrand et al., 2013; May et al., 2013) and potentially contributes to the radiative forcing in the glacierized region.

The TP has the largest number of glaciers at moderate elevations. Most of the glaciers on the TP are experiencing intensive retreat because of increases in temperature (Kang et al., 2010; Yao et al., 2012; Yao, 2004a; Kang et al., 2015; Zhang et al., 2015) and anthropogenic carbonaceous particle deposition (Ming et al., 2008; Xu et al., 2009; Qu et al., 2014; Kaspari et al., 2014). However, to date, no study has quantitatively evaluated the light absorption characteristics of DOC in the glacierized regions on the TP, despite some investigations of concentrations and sources of DOC (Spencer et al., 2014; Yan et al., 2015). The primary results of these studies have shown that DOC concentrations in snowpits in the northern TP are higher than those in the southern TP (Yan et al., 2015). In addition, a large fraction of the ancient DOC in the glaciers in the southern TP has high bioavailability characteristics (Spencer et al., 2014). However, knowledge of DOC in TP glaciers remains lacking due to the large area and diverse environments of the TP and the relatively limited samples and studies. Therefore, numerous snow (n=67), ice (n=42) and proglacial streamwater samples (n=201) were collected from a typical glacier in the northeastern TP (Laohugou glacier No. 12) based on the preliminary research of snowpit samples (Yan et al., 2015) (Table 1, Fig. 1). The concentrations of DOC and major ions (Ca^{2+}, Mg^{2+}, Na^{+}, K^{+}, NH_4^{+}, Cl^{-}, NO_3^{-} and SO_4^{2-}) and DOC light absorbance were measured to comprehensively investigate the sources, light absorption properties and carbon dynamics in this glacierized region to provide a basis for the study of DOC across the TP and other regions in the future.

2 Methodology

2.1 Study area and sampling site

Laohugou glacier No. 12 (LHG glacier) (39°05'-40'N, 96°07'-97°04'E 4260-5481 m) is the largest mountain glacier (9.85 km, 20.4 km^2) in the Qilian Mountains located on the northeastern edge of the TP (Du et al., 2008; Dong et al., 2014a). It is divided into two part of western and eastern branch at the

98 elevation of 4560 m a.s.l (Dong et al., 2014a). This glacier is surrounded by large arid and semi-arid
99 regions (sandy deserts and the Gobi desert) (Fig. 1). The area of the glacier covers approximately 53.6 %
100 of the entire LHG glacier basin (Du et al., 2008; Li et al., 2012).

101 LHG glacier features typical continental and arid climate characteristics (Li et al., 2012; Zhang et
102 al., 2012b). Precipitation occurs mainly from May to September, accounting for over 70 % of the total
103 annual precipitation (Zhang et al., 2012b). The monthly mean air temperatures in the ablation zone of
104 the glacier range from -18.4 ℃ in December to 3.4 ℃ in July (Li et al., 2012). Like other glaciers on the
105 TP, LHG glacier has been experiencing significant thinning and shrinkage at an accelerated rate since
106 the mid-1990s (Du et al., 2008; Zhang et al., 2012b).

107 **2.2 Sample collection**

108 Two snowpits were dug in 2014 and 2015 almost in the same site in the accumulation zone of
109 LHG glacier. In total, 15 and 23 snow samples were collected in 2014 and 2015, respectively, at a
110 vertical resolution of 5 cm for each snowpit. Moreover, 29 surface snow and 42 surface ice samples
111 were collected along the eastern tributary at an approximate elevation interval of 50 or 100 m from the
112 terminus to the accumulation zone, and 201 proglacial streamwater samples were collected at the gauge
113 station during the melting period (Fig. 1, Table 1). The concentrations of glacier DOC have been
114 observed to be very low and prone to contamination, causing an overestimation of DOC concentrations
115 (Legrand et al., 2013). Therefore, before sample collection, polycarbonate bottles were firstly cleaned
116 by ultrapure water for three times, then soaked into 1 M HCl for 24 h (Spencer et al., 2009), and rinsed
117 three times using ultrapure water, finally soaked into ultrapure water for over 24 h; during the whole
118 sampling procedure, snow samples were collected directly into 125-mL pre-cleaned bottles, surface ice
119 (0-3 cm and 3-5 cm) samples were collected using an ice axe directly into polycarbonate bottles after
120 crushing, while proglacial streamwater samples were filtered immediately after collection before
121 putting into bottles. All ice and snow sample were filtered as soon as possible after they were melted.
122 During all the processes, the person who takes charge of sample collection should not touch any other
123 things to avoid contamination. Meanwhile, at least one blank was made for every sampling process to
124 confirm that the contamination was low (Table S1). Meanwhile, another batch of samples were also
125 collected for BC concentration measurement following the protocol discussed in detail in our earlier
126 work (Qu et al., 2014); these results will be presented in another article. In order to evaluate DOC
127 release of the entire TP, DOC concentrations of proglacial streamwater samples of other five glaciers in

monsoon and non-monsoon seasons were measured, respectively (Fig. 1, Table S2).

All the collected samples were kept frozen and in the dark in the field, during transportation and in the laboratory until analysis. In addition, four dust fall samples from Dunhuang, a desert location (39 °53'-41 °35'N, 92 °13'-93 °30'E) – potential source region of the dust deposited on LHG glacier – were collected to compare the light absorption characteristics of dust-sourced DOC to those of the snowpit and ice samples. Mineral and elemental composition of desert sands of west China are homogenized by aeolian activity (Hattori et al., 2003), so that the dust samples collected in this study are representative of desert sourced dust in west China.

2.3 Laboratory analyses

2.3.1 Concentration measurements of DOC and major ions

DOC concentrations were determined using a TOC-5000A analyzer (Shimadzu Corp, Kyoto, Japan) after the collected samples were filtered through a PTFE membrane filter with 0.45-μm pore size (Macherey–Nagel) (Yan et al., 2015). The detection limit of the analyzer was 15 μg L^{-1}, and the average DOC concentration of the blanks was 32 ± 7 μg L^{-1}, demonstrating that contamination can be ignored during the pre-treatment and analysis processing of these samples (Table S1). The major cations (Ca^{2+}, Mg^{2+}, Na^{+}, K^{+} and NH_4^{+}) and major anions (Cl^{-}, NO_3^{-} and SO_4^{2-}) were measured using a Dionex-6000 Ion Chromatograph and a Dionex-3000 Ion Chromatograph (Dionex, USA), respectively. The detection limit was 1 μg L^{-1}, and the standard deviation was less than 5 % (Li et al., 2007; Li et al., 2010). The average ion concentrations of the blank were very low and could be ignored (Na^{+}, K^{+}, Mg^{2+}, F^{+}, SO_4^{2-}, Cl^{-}, NO_3^{-} < 1 μg L^{-1}; NH_4^{+} = 1.4 μg L^{-1}; Ca^{2+} = 1.2 μg L^{-1}).

2.3.2 Light absorption measurements

The light absorption spectra of DOC were measured using an ultraviolet-visible absorption spectrophotometer (SpectraMax M5, USA), scanning wavelengths from 200-800 nm at a precision of 5 nm. The mass absorption cross section (MAC) was calculated based on the Lambert-Beer Law (Bosch et al., 2014; Kirillova et al., 2014a; Kirillova et al., 2014b):

$$\mathrm{MAC_{DOC}} = \frac{-\ln|\frac{I}{I0}|}{\mathrm{C.L}} = \frac{\mathrm{A}}{\mathrm{C.L}} \times \ln(10) \qquad (1)$$

where I_0 and I are the light intensities of the transmitted light and incident light, respectively; A is the

absorbance derived directly from the spectrophotometer; C is the concentration of DOC; and L is the absorbing path length (1 cm).

In order to investigate the wavelength dependence of DOC light absorption characteristics, the Absorption Ångström Exponent (AAE) was fitted by the following equation (Kirillova et al., 2014b;Kirillova et al., 2014a):

$$\frac{A(\lambda_1)}{A(\lambda_2)} = \left(\frac{\lambda_2}{\lambda_1}\right)^{AAE} \quad (2)$$

AAE values were fitted from the wavelengths of 330 to 400 nm; within this wavelength range, light absorption by other inorganic compounds can be avoided (such as nitrate) (Cheng et al., 2011).The radiative forcing caused by BC has been widely studied (Kaspari et al., 2014; Qu et al., 2014; Ming et al., 2013). Therefore, in this study, using a simplistic model (the following algorithm), the amount of solar radiation absorbed by DOC compared to BC was estimated:

$$f = \frac{\int_{300}^{2500} I_0(\lambda)\cdot\left\{1-e^{-(MAC_{365}\left(\frac{365}{\lambda}\right)^{AAE_{DOC}}\cdot C_{DOC}\cdot h_{ABL})}\right\}d\lambda}{\int_{300}^{2500} I_0(\lambda)\cdot\left\{1-e^{-(MAC_{550}\left(\frac{550}{\lambda}\right)^{AAE_{BC}}\cdot C_{EC}\cdot h_{ABL})}\right\}d\lambda} \quad (3)$$

where λ is the wavelength; $I_0(\lambda)$ is the clear sky solar emission spectrum determined using the Air Mass 1 Global Horizontal (AM1GH) irradiance model (Levinson et al., 2010); MAC_{365} and MAC_{550} are the mass absorption cross section of DOC at 365 nm and mass absorption cross section of BC at 550 nm, respectively; h_{ABL} is the vertical height of the atmospheric boundary layer; and AAE_{DOC} and AAE_{BC} are the Absorption Ångström Exponents (AAEs) of DOC and BC. In this simplistic model, following a previous study, we used $MAC_{550} = 7.5 \pm 1.2$ $m^2 g^{-1}$ (Bond and Bergstrom, 2006), and AAE for BC was set as 1, while h_{ABL} was set to 1000 m, which has little influence on the integration from the wavelengths of 300 - 2500 nm (Kirillova et al., 2013; Bosch et al., 2014; Kirillova et al., 2014a; Kirillova et al., 2014b). It is obvious that the value of "f" is closely connected with relative concentrations between DOC and BC.

2.3.3 *In situ* DOC bioavailability experiment

The bioavailability experiment was conducted from August 17th to 31st, 2015, at the glacier terminus during fieldwork. In brief, surface ice samples were collected in pre-combusted (550 ℃, 6 h) aluminum basins and melted in the field. The melted samples were filtered through pre-combusted

glass fiber filters (GF/F 0.7 μm) into 12 pre-cleaned 125-mL polycarbonate bottles and wrapped with three layers of aluminum foil to avoid solar irradiation. Two samples were refrigerated immediately after filtering to obtain initial DOC concentrations; the others were placed outside at the terminus of the glacier, and 2 samples were refrigerated every 3 days to get corresponding DOC values. The BDOC was calculated based on the discrepancies between the initial and treated samples.

3 Results and discussion

3.1 DOC concentrations and bioavailability

3.1.1 Snowpits

LHG glacier is surrounded by arid and semi-arid regions and frequently influenced by strong dust storms (Dong et al., 2014b) (Fig. 1). Therefore, heavy desert sourced mineral dust deposition contributes to high DOC concentrations on LHG glacier. The average DOC concentration of the snowpit samples was 332 ± 132 μg L^{-1} (Fig. 2), with values ranging from 124 μg L^{-1} to 581. μg L^{-1} (Fig. 3). The highest values appeared in the dirty layers (Fig. 3), similar to the pattern observed in the Greenland summit (Hagler et al., 2007) and glaciers in the southern TP (Xu et al., 2013), indicating that DOC concentrations were mainly influenced by dust deposition in this region in addition to the potential microbial activities (Anesio et al., 2009). Spatially, our results were higher than those of Xiaodongkemadi glacier on Mountain Tanggula (TGL) in the middle TP and East Rongbu glacier on Mount Everest (EV) in the southern TP (Fig. 1) (Yan et al., 2015) but similar to the mercury distribution on the TP (Zhang et al., 2012a). Moreover, the DOC concentrations on LHG glacier were also higher than those of Alaskan glaciers (Stubbins et al., 2012) and the Greenland summit (Hagler et al., 2007) (Table 2).

3.1.2 Surface snow and ice

The average DOC concentration in LHG glacier surface snow was significantly lower than that in surface ice because more impurities are present in the latter (Fig. 2). Like those of the snowpits, DOC concentrations in the glacier surface ice (Fig. 2) were higher than those in the southern TP (Nyainqentanglha glacier) (Spencer et al., 2014) and subsurface ice (0.5 m beneath the glacier surface) in a European Alpine glacier (Singer et al., 2012) (Table 2) but comparable to that in the surface ice of the Antarctic ice sheet (Hood et al., 2015). However, the DOC concentrations in surface snow (Table 2) were higher than those in the Greenland ice sheet (Hagler et al., 2007), mainly due to the heavy dust load of LHG glacier. No significant relationship was found between DOC concentration and elevation

for either the surface snow or ice (Fig. S1), suggesting no "altitude effect" on DOC in this glacier. This finding is similar to the mercury distribution pattern in surface snow of this glacier (Huang et al., 2014). Therefore, the distributions of DOC concentrations in the glacier surface snow and ice were influenced by complicated factors, such as different slopes (Hood and Scott, 2008) and cryoconite holes. Furthermore, DOC concentrations of snow and ice of this glacier were within the range of previously reported values for glacieried regions outside the TP.

3.1.3 DOC bioavailability

Previous studies conducted under controlled conditions (stable temperature) have shown that glacier-derived DOC is more bioavailable than terrestrial-derived DOC (Hood et al., 2009; Fellman et al., 2010; Spencer et al., 2014). Our results showed that the amount of DOC being consumed decreased exponentially over time ($R^2 = 0.98$) (Fig. 4), with approximately 26.7 % (from 417μg L^{-1} to 306 μg L^{-1}) degraded within 15 days during the experiment (average temperature: 3.8 ± 3.7 ℃; range: -4.8-11.4 ℃). The BDOC reached 46.3 % if the experiment duration was extended to 28 days, according to the equation derived from the 15-day experiment (Fig. 4). Despite different incubation conditions, this finding agrees well with the reports of BDOC from a glacier in the southern TP (28-day dark incubation at 20 ℃, 46-69 % BDOC）(Spencer et al., 2014) and European Alpine glaciers (50-day dark incubation at 4 ℃, 59±20 % BDOC) (Singer et al., 2012). Therefore, the previous results obtained in the laboratory closely reflect the real situation and can be used to estimate the bioavailability of glacier-derived DOC.

3.2 Sources of snowpit DOC

The sources of glacier DOC are diverse and include autochthonous or *in situ* biological activities (Anesio et al., 2009; Bellas et al., 2013), allochthonous carbon derived from overridden soils and vegetation in subglacial systems (Bhatia et al., 2010); terrestrial inputs (DOC deposition from vascular plants and dust) (Singer et al., 2012) and anthropogenic sources (fossil fuel and biomass combustion) (Stubbins et al., 2012; Spencer et al., 2014). Research on glacier microbial activity suggests that globally only cryoconite holes can potentially fix about 64 Gg C per year (Anesio et al., 2009). Moreover, viral induced mortality at the cost of heterotrophic bacterial community plays a dominant role in carbon cycle and other nutrients transformation in supraglacier ecosystems (Bellas et al., 2013). In this study, major ions were adopted as indicators to investigate the potential sources of snowpit DOC,

because the sources of major ions in snowpit samples from Tibetan glaciers have been investigated in detail (Kang et al., 2002; Kang et al., 2008; Wu et al., 2011; Yan et al., 2015). Moreover, the profiles of DOC in two snowpits varied with the dust content, DOC concentration of dust layer was much higher than that of clean layers. Furthermore, it was found that DOC and Ca^{2+} (a typical indicator of mineral dust (Yao, 2004b)) were significantly related ($R^2 = 0.84$, Fig. S2), suggesting that the major source of DOC was desert sourced mineral dust, which is consistent with the previous DOC source investigations of snowpits on this glacier (Yan et al., 2015). In addition, the combined study of geochemistry and backward trajectories for LHG glacier showed that the dust particles on the glacier were mainly derived from the deserts to the west and north of the study area (Dong et al., 2014a; Dong et al., 2014b).

3.3 Light absorption characteristics of DOC

3.3.1 AAE

The Absorption Ångström Exponent (AAE) is generally used to characterize the spectral dependence of the light absorption of DOC, which is important input data for radiative forcing calculations. The fitted $AAE_{330\text{-}400}$ values ranged from 1.2 to 15.2 (5.0 ± 5.9) for snow samples and from 0.3 to 8.4 (3.4 ± 2.7) for ice samples (Fig. S4). The relatively low $AAE_{330\text{-}400}$ values of the ice indicated that the DOC experienced strong photobleaching due to long-duration exposure to solar irradiation. Previous studies have found that the AAE values of brown carbon in aged aerosols (Zhao et al., 2015) and secondary organic aerosols (SOAs) (Lambe et al., 2013) were much lower compared to that of the primary values. Therefore, the large divergence in AAE values might suggest different chemical compositions of DOC due to multiple possibilities, such as different sources and photobleaching processes. Regardless, the average AAE value of the snow samples was comparable to that of atmospheric aerosols in urban areas in South Asia (New Delhi, India) (Kirillova et al., 2014b) (Table 2). In general, the $AAE_{330\text{-}400}$ values had a negative relationship with MAC_{365}, especially in the ice samples (Fig. S4), suggesting that stronger absorbing DOC might contribute to lower AAE values, which was also found in other aerosol studies (Chen and Bond, 2010; Bosch et al., 2014; Kirillova et al., 2014b).

3.3.2 MAC_{365}

The mass absorption cross section at 365 nm (MAC_{365}) for DOC is another input data point for the radiative forcing calculation. The light absorption ability at 365 nm is selected to avoid interferences of non-organic compounds (such as nitrate) and to be consistent with previous investigations (Hecobian et

al., 2010; Cheng et al., 2011). The MAC_{365} was 1.4 ± 0.4 m^2 g^{-1} in snow and 1.3 ± 0.7 m^2 g^{-1} in glacier ice (Fig. S4), both of which were higher than those of water soluble organic carbon in outflow in northern China (Kirillova et al., 2014a) and a receptor island in the Indian Ocean (Bosch et al., 2014). Meanwhile, the values were comparable to DOC concentrations in typical urban aerosols associated with biomass combustion in winter in Beijing, China (Cheng et al., 2011) and in New Delhi, India (Kirillova et al., 2014b) (Table 3). The MAC values for DOC from different sources vary widely. Normally, the MAC_{365} of DOC derived from biomass combustion can be as high as 5 m^2 g^{-1} (Kirchstetter, 2004) (Table 3). Correspondingly, the values for SOAs can be as low as 0.001-0.088 m^2 g^{-1} (Lambe et al., 2013). Due to the remote location of LHG glacier, it was considered that the snowpit DOC should be SOAs with low MAC_{365} values; however, the high MAC_{365} value of the snowpit DOC indicated that DOC may not be entirely derived from SOAs. Here, it was proposed that mineral dust-sourced DOC caused the high MAC_{365} values in the snowpit samples. For instance, the light absorption characteristics of DOC from both snowpit and ice showed similar patterns to those of water soluble organic carbon in dust from the adjacent deserts, further indicating that LHG glacier DOC was transported via desert sourced mineral dust and shared similar light absorption characteristics (Fig. 5). Moreover, the difference in light absorption characteristics (especially for wavelengths larger than 400 nm) between snow/ice samples and aerosols in Beijing, China, also indicated different sources (Fig. 5). Light absorbance was significantly correlated with DOC concentrations in both snow and ice samples (Fig. S3), indicating that DOC was one of the absorption factors. Nevertheless, the MAC_{365} values of surface ice (0-3 cm) were lower than those of subsurface layers (3-5 cm), despite its higher DOC concentrations (Fig. 6), reflecting stronger DOC photobleaching in the surface ice due to the direct exposure to solar irradiation.

3.3.3 Radiative forcing of DOC relative to BC

The radiative forcing contributed by water soluble organic carbon relative to BC in aerosols has been proposed to be as high as 2-10 % (Kirillova et al., 2013; Kirillova et al., 2014a). Furthermore, it was estimated that brown carbon accounts for a higher ratio of 20 % of the direct radiative forcing of aerosols at the top of the atmosphere because BC concentrations decrease faster than brown carbon in the high-altitude atmosphere (Liu et al., 2014).

Our results showed that the relative radiative forcing caused by DOC relative to BC ranged from 2.1 % to 30.4 % (9.5 ± 8.4 %) for snowpit samples and from 0.01 % to 0.5 % (0.1 ± 0.1%) for surface

ice samples (Fig. S4). The high radiative forcing ratio of snowpit samples was caused by its higher DOC/BC (0.65) than that of surface ice (0.012) (Fig. S5), and the low ratio of DOC/BC in surface ice was caused by enrichment of BC in surface glacier ice during the intensive ablation period (Xu et al., 2009). Snowpit samples can be approximately considered to be fresh snow; thus, it is concluded that radiative forcing caused by DOC is a non-ignorable contributor in addition to BC in reducing the albedo of a glacier when the glacier is covered by fresh snow.

3.4 DOC export during the melt season

The two-year average discharge-weighted DOC concentration was 238 ± 96 μg L^{-1} during the melting period, comparable with the proglacial streamwater of Mount Nyainqentanglha glacier in the southern TP (Spencer et al., 2014). Seasonally, high DOC concentrations appeared during the low discharge periods (May to July and September to October) (Fig. 7), suggesting that DOC concentrations were slightly enriched to some extent. However, there were no clear diurnal variations in the DOC concentrations with the discharge, suggesting that the discharge from different parts of the glacier was well mixed at the glacier terminus (Fig. S6).

The seasonal variations in DOC flux were similar to those of the discharge (Fig. 7), indicating that discharge (rather than DOC concentrations) played a dominant role in the DOC mass flux. Hence, the majority of the glacier DOC export occurred during the summer melting season. Over the whole melting season, the annual flux of DOC from LHG glacier was 192 kg km^{-2} yr^{-1}, with peak DOC fluxes from mid-late July to late August (70 % of the annual flux). Combined with the value of BDOC determined above, at least 3211 kg C yr^{-1} was ready to be decomposed and returned to the atmosphere as CO_2 within one month of its release, producing positive feedback in the global warming process.

When it comes to the entire TP, it is obvious that proglacial streamwater DOC concentrations (Table S2) showed similar spatial variation to that of snowpit DOC (Li et al., 2016), with high and low value appeared at north and south TP, respectively, reflecting good succession of proglacial streamwater DOC concentration to that of snowpit samples. Therefore, it was calculated that DOC flux in proglacial streamwater of the entire TP glacier was around 12.7-13.2 Gg C (Gg = 10^9 g) based on average proglacial streamwater DOC concentration of 193 μg L^{-1} (Table S2) and annual glacial meltwater runoff in China of 66-68.2 km^3 (Xie et al., 2006), which is higher than that of DOC deposition (5.6 Gg C) at glacial region of the TP (Li et al., 2016), agree well with the negative water balance of the glaciers of the TP. Therefore, the TP glaciers can be considered as a carbon source under

present environment condition.

4 Conclusions and implications

The concentrations and light absorption characteristics of DOC on a typical glacier in the northern TP were reported in this study. The mean DOC concentrations of snowpit samples, fresh snow, surface ice and proglacial streamwater were 332 ± 132 μg L^{-1}, 229 ± 104 μg L^{-1}, 426 ± 270 μg L^{-1} and 238 ± 96 μg L^{-1}, respectively. These values were slightly higher or comparable to those of other regions, such as the European Alps and Alaska (Singer et al., 2012; Fellman et al., 2015). DOC in the snowpit samples was significantly correlated with Ca^{2+}, a typical cation in mineral dust, indicating that mineral dust transported from adjacent arid regions made important contributions to DOC of the studied glacierized regions except autochthonous or *in situ* biological activities. In addition, the light absorption profile of the snowpit DOC was similar to that of dust from potential source deserts, providing further evidence of the influence of desert sourced mineral dust on snowpit DOC. Based on the previous published radiative forcing data of black carbon in snowpit of LHG (Ming et al., 2013), for the first time, it is estimated that the radiative forcing caused by snowpit DOC was 0.43 W m^{-2}, accounting for around 10 % of the radiative forcing caused by BC. Therefore, in addition to BC, DOC is also an important agent in terms of absorbing solar radiation in glacierized regions, especially when the glacier is covered by fresh snow. It has also been proven that water-insoluble organic carbon has stronger light absorption ability (Chen and Bond, 2010). Therefore, the total contribution of OC to light absorption in glacierized regions should be higher, which requires further study in the future. Wet deposition is the most effective way of removing carbonaceous matter from the atmosphere (Vignati et al., 2010), and the removal ratio of OC in remote areas is almost the same as that of BC after long-range transport from source regions (Garrett et al., 2011). Because snowpit samples directly reflect the wet and dry deposition of carbonaceous matter, it is assumed that the contribution of radiative forcing for water soluble organic carbon relative to BC in the atmosphere in glacierized regions should be close to that of the snowpit samples in this study.

Because proglacial streamwater from different parts of the glacier is well mixed, no clear diurnal variations in DOC concentrations have been found. Combined with discharge and the corresponding DOC concentration, it was calculated that approximate 192.0 kg km^{-2} yr^{-1} of DOC was released from LHG glacier. It was also calculated that approximately 46.3 % of the DOC could be decomposed within 28 days; thus, 3,211 kg C yr^{-1} would return to the atmosphere as CO_2, producing positive

feedback in the warming process. Although the flux of DOC from the studied glacier is small, when it comes to the entire TP DOC flux from glaciers of the total TP was around 12.7-13.2 Gg C.

Acknowledgements. This study was supported by the National Nature Science Foundation of China (41225002, 41271015, 41121001), State Key Laboratory of Cryospheric Science (SKLCS-ZZ-2015-10 and SKLCS-OP-2014-05) and the Academy of Finland (decision number 268170). The authors acknowledge the staff of the Qilian Shan Station of Glaciology and Ecological Environment, Chinese Academy of Science.

References

Andreae, M. and Gelencsér, A.: Black carbon or brown carbon? The nature of light-absorbing carbonaceous aerosols, Atmos. Chem. Phys., 6, 3131-3148, 2006.

Anesio, A. M., Hodson, A. J., Fritz, A., Psenner, R., and Sattler, B.: High microbial activity on glaciers: importance to the global carbon cycle, Global Change Biol., 15, 955-960, 2009.

Anesio, A. M. and Laybourn-Parry, J.: Glaciers and ice sheets as a biome, Trends Ecol. Evol., 27, 219-225, 2012.

Antony, R., Grannas, A. M., Willoughby, A. S., Sleighter, R. L., Thamban, M., and Hatcher, P. G.: Origin and sources of dissolved organic matter in snow on the East Antarctic ice sheet, Environ. Sci. Technol., 48, 6151-6159, 2014.

Antony, R., Mahalinganathan, K., Thamban, M., and Nair, S.: Organic Carbon in Antarctic Snow: Spatial Trends and Possible Sources, Environ. Sci. Technol., 45, 9944-9950, 2011.

Bhatia, M. P., Das, S. B., Longnecker, K., Charette, M. A., and Kujawinski, E. B.: Molecular characterization of dissolved organic matter associated with the Greenland ice sheet, Geochim. Cosmochim. Acta., 74, 3768-3784, 2010.

Bhatia, M. P., Das, S. B., Xu, L., Charette, M. A., Wadham, J. L., and Kujawinski, E. B.: Organic carbon export from the Greenland ice sheet, Geochim. Cosmochim. Acta., 109, 329-344, 2013.

Bond, T. C., and Bergstrom, R. W.: Light Absorption by Carbonaceous Particles: An Investigative Review, Aerosol Sci. Technol., 40, 27-67, 10.1080/02786820500421521, 2006.

Bosch, C., Andersson, A., Kirillova, E. N., Budhavant, K., Tiwari, S., Praveen, P., Russell, L. M., Beres, N. D., Ramanathan, V., and Gustafsson, Ö.: Source‐diagnostic dual‐isotope composition and optical properties of water‐soluble organic carbon and elemental carbon in the South Asian outflow intercepted over the Indian Ocean, J. Geophys. Res. Atmos., 119, 11,743-711,759, 2014.

Chen, Y. and Bond, T. C.: Light absorption by organic carbon from wood combustion, Atmos. Chem. Phys., 10, 1773-1787, 2010.

Cheng, Y., He, K. B., Zheng, M., Duan, F. K., Du, Z. Y., Ma, Y. L., Tan, J. H., Yang, F. M., Liu, J. M., Zhang, X. L., Weber, R. J., Bergin, M. H., and Russell, A. G.: Mass absorption efficiency of elemental carbon and water-soluble organic carbon in Beijing, China, Atmos. Chem. Phys., 11, 11497-11510, 2011.

Dong, Z., Qin, D., Chen, J., Qin, X., Ren, J., Cui, X., Du, Z., and Kang, S.: Physicochemical impacts of dust particles on alpine glacier meltwater at the Laohugou Glacier basin in western Qilian Mountains, China, Sci. Total Environ., 493, 930-942, 2014a.

Dong, Z., Qin, D., Kang, S., Ren, J., Chen, J., Cui, X., Du, Z., and Qin, X.: Physicochemical characteristics and sources of atmospheric dust deposition in snow packs on the glaciers of western Qilian Mountains, China, Tellus B, 66, 2014b.

Du, W., Qin, X., Liu, Y. S., and Wang, X. F.: Variation of Laohugou Glacier No. 12 in Qilian Mountains, Journal of Glaciology and Geocryology, 30, 373-379, 2008 (in Chinese with English abstract).

Fellman, J. B., Hood, E., Raymond, P. A., Stubbins, A., and Spencer, R. G. M.: Spatial Variation in the Origin of Dissolved Organic Carbon in Snow on the Juneau Icefield, Southeast Alaska, Environ. Sci. Technol., doi: 10.1021/acs.est.5b02685, 2015.

Fellman, J. B., Spencer, R. G. M., Hernes, P. J., Edwards, R. T., D'Amore, D. V., and Hood, E.: The impact of glacier runoff on the biodegradability and biochemical composition of terrigenous dissolved organic matter in near-shore marine ecosystems, Mar. Chem., 121, 112-122, 2010.

Garrett, T. J., Brattström, S., Sharma, S., Worthy, D. E. J., and Novelli, P.: The role of scavenging in the seasonal transport of black carbon and sulfate to the Arctic, Geophys. Res. Lett., 38, L16805, doi:10.1029/2011GL048221, 2011.

Hagler, G. S. W., Bergin, M. H., Smith, E. A., Dibb, J. E., Anderson, C., and Steig, E. J.: Particulate and water-soluble carbon measured in recent snow at Summit, Greenland, Geophys. Res. Lett., 34, L16505, doi:10.1029/2007GL030110, 2007.

Hattori, Y., Suzuki, K., Honda, M., and Shimizu, H.: Re-Os isotope systematics of the Taklimakan Desert sands, moraines and river sediments around the Taklimakan Desert, and of Tibetan soils, Geochim. Cosmochim. Acta., 67, 1203-1213, 2003.

Hecobian, A., Zhang, X., Zheng, M., Frank, N., Edgerton, E. S., and Weber, R. J.: Water-Soluble Organic Aerosol material and the light-absorption characteristics of aqueous extracts measured over the Southeastern United States, Atmos. Chem. Phys., 10, 5965-5977, 2010.

Hood, E., Battin, T. J., Fellman, J., O'Neel, S., and Spencer, R. G. M.: Storage and release of organic carbon from glaciers and ice sheets, Nat. Geosci., 8, 91-96, 2015.

Hood, E., Fellman, J., Spencer, R. G., Hernes, P. J., Edwards, R., D'Amore, D., and Scott, D.: Glaciers as a source of ancient and labile organic matter to the marine environment, Nature, 462, 1044-1047, 2009.

Hood, E. and Scott, D.: Riverine organic matter and nutrients in southeast Alaska affected by glacial coverage, Nat. Geosci, 1, 583-587, 2008.

Huang, J., Kang, S., Guo, J., Sillanpää, M., Zhang, Q., Qin, X., Du, W., and Tripathee, L.: Mercury distribution and variation on a high-elevation mountain glacier on the northern boundary of the Tibetan Plateau, Atmos. Environ., 96, 27-36, 2014.

Jacob, T., Wahr, J., Pfeffer, W. T., and Swenson, S.: Recent contributions of glaciers and ice caps to sea level rise, Nature, 482, 514-518, 2012.

Kang, S., Mayewski, P. A., Qin, D., Yan, Y., Hou, S., Zhang, D., Ren, J., and Kruetz, K.: Glaciochemical records from a Mt. Everest ice core: relationship to atmospheric circulation over Asia, Atmos. Environ., 36, 3351-3361, 2002.

Kang, S., Wang, F., Morgenstern, U., Zhang, Y., Grigholm, B., Kaspari, S., Schwikowski, M., Ren, J., Yao, T., Qin, D., and Mayewski, P. A.: Dramatic loss of glacier accumulation area on the Tibetan Plateau revealed by ice core tritium and mercury records, The Cryosphere, 9, 1213-1222, 2015.

Kang, S., Xu, Y., You, Q., Flügel, W.-A., Pepin, N., and Yao, T.: Review of climate and cryospheric change in the Tibetan Plateau, Environ. Res. Lett., 5, 015101, doi:10.1088/1748-9326/5/1/015101, 2010.

Kang, S. C., Huang, J., and Xu, Y. W.: Changes in ionic concentrations and δ18O in the snowpack of Zhadang glacier, Nyainqentanglha mountain, southern Tibetan Plateau, Ann. Glaciol., 49, 127-134, 2008.

Kaspari, S., Painter, T. H., Gysel, M., Skiles, S. M., and Schwikowski, M.: Seasonal and elevational variations of black carbon and dust in snow and ice in the Solu-Khumbu, Nepal and estimated radiative forcings, Atmos. Chem. Phys., 14, 8089-8103, 2014.

Kirchstetter, T. W.: Evidence that the spectral dependence of light absorption by aerosols is affected by organic carbon, J. Geophys. Res., 109, D21208, doi:10.1029/2004JD004999, 2004.

Kirillova, E. N., Andersson, A., Han, J., Lee, M., and Gustafsson, Ö.: Sources and light absorption of water-soluble brown carbon aerosols in the outflow from northern China, Atmos. Chem. Phys. Discuss., 13, 19625-19648, 2013.

Kirillova, E. N., Andersson, A., Han, J., Lee, M., and Gustafsson, Ö.: Sources and light absorption of water-soluble organic carbon aerosols in the outflow from northern China, Atmos. Chem. Phys., 14, 1413-1422, 2014a.

Kirillova, E. N., Andersson, A., Tiwari, S., Srivastava, A. K., Bisht, D. S., and Gustafsson, Ö.: Water-soluble organic carbon aerosols during a full New Delhi winter: Isotope-based source apportionment and optical properties, J. Geophys. Res. Atmos., 119, 3476-3485, 2014b.

Lambe, A. T., Cappa, C. D., Massoli, P., Onasch, T. B., Forestieri, S. D., Martin, A. T., Cummings, M. J., Croasdale, D. R., Brune, W. H., and Worsnop, D. R.: Relationship between oxidation level and optical properties of secondary organic aerosol, Environ. Sci. Technol., 47, 6349-6357, 2013.

Lawson, E. C., Wadham, J. L., Tranter, M., Stibal, M., Lis, G. P., Butler, C. E. H., Laybourn-Parry, J., Nienow, P., Chandler, D., and Dewsbury, P.: Greenland Ice Sheet exports labile organic carbon to the Arctic oceans, Biogeosci., 11, 4015-4028, 2014.

Legrand, M., Preunkert, S., Jourdain, B., Guilhermet, J., Fain, X., Alekhina, I., and Petit, J. R.: Water-soluble organic carbon in snow and ice deposited at Alpine, Greenland, and Antarctic sites: a critical review of available data and their atmospheric relevance, Clim. Past Discuss., 9, 2357-2399, 2013.

Levinson, R., Akbari, H., and Berdahl, P.: Measuring solar reflectance—Part I: Defining a metric that accurately predicts solar heat gain, Sol. Energy, 84, 1717-1744, 2010.

Li, C., Kang, S., Zhang, Q., and Kaspari, S.: Major ionic composition of precipitation in the Nam Co region, Central Tibetan Plateau, Atmos. Res., 85, 351-360, 2007.

Li, C., Chen, P., Kang, S., Yan, F., Li, X., Qu, B., and Sillanpää, M.: Carbonaceous matter deposition in the high glacial regions of the Tibetan Plateau, Atmos. Environ., 141, 203-208, 2016.

Li, J., Qin, X., Sun, W., zhang, M., and Yang, J.: Analysis on Micrometerological Characteristic in the Surface Layer of Laohugou Glacier No.12 Qilian Mountains, Plateau Meteorology, 31, 370-379, 2012.

Li, Z., Li, H., Dong, Z., and Zhang, M.: Chemical characteristics and environmental significance of fresh snow deposition on Urumqi Glacier No. 1 of Tianshan Mountains, China, Chinese Geographical Science, 20, 389-397, 2010.

Liu, J., Scheuer, E., Dibb, J., Ziemba, L. D., Thornhill, K., Anderson, B. E., Wisthaler, A., Mikoviny, T., Devi, J. J., and Bergin, M.: Brown carbon in the continental troposphere, Geophys. Res. Lett., 41, 2191-2195, 2014.

May, B., Wagenbach, D., Hoffmann, H., Legrand, M., Preunkert, S., and Steier, P.: Constraints on the major sources of dissolved organic carbon in Alpine ice cores from radiocarbon analysis over the bomb - peak period, J. Geophys. Res. Atmos., 118, 3319-3327, 2013.

Ming, J., Cachier, H., Xiao, C., Qin, D., Kang, S., Hou, S., and Xu, J.: Black carbon record based on a shallow Himalayan ice core and its climatic implications, Atmos. Chem. Phys., 8, 1343-1352, 2008.

Ming, J., Xiao, C., Du, Z., and Yang, X.: An overview of black carbon deposition in High Asia glaciers and its impacts on radiation balance, Adv. Water Resour., 55, 80-87, 2013.

Qu, B., Ming, J., Kang, S. C., Zhang, G. S., Li, Y. W., Li, C. D., Zhao, S. Y., Ji, Z. M., and Cao, J. J.: The decreasing albedo of the Zhadang glacier on western Nyainqentanglha and the role of light-absorbing impurities,

Atmos. Chem. Phys., 14, 11117-11128, 2014.

Singer, G. A., Fasching, C., Wilhelm, L., Niggemann, J., Steier, P., Dittmar, T., and Battin, T. J.: Biogeochemically diverse organic matter in Alpine glaciers and its downstream fate, Nat. Geosci., 5, 710-714, 2012.

Spencer, R. G., Stubbins, A., Hernes, P. J., Baker, A., Mopper, K., Aufdenkampe, A. K., Dyda, R. Y., Mwamba, V. L., Mangangu, A. M., and Wabakanghanzi, J. N.: Photochemical degradation of dissolved organic matter and dissolved lignin phenols from the Congo River, J. Geophys. Res. Biogeosci., 114, 2009.

Spencer, R. G. M., Guo, W., Raymond, P. A., Dittmar, T., Hood, E., Fellman, J., and Stubbins, A.: Source and biolability of ancient dissolved organic matter in glacier and lake ecosystems on the Tibetan Plateau, Geochim. Cosmochim. Acta, 142, 64-74, 2014.

Stubbins, A., Hood, E., Raymond, P. A., Aiken, G. R., Sleighter, R. L., Hernes, P. J., Butman, D., Hatcher, P. G., Striegl, R. G., Schuster, P., Abdulla, H. A. N., Vermilyea, A. W., Scott, D. T., and Spencer, R. G. M.: Anthropogenic aerosols as a source of ancient dissolved organic matter in glaciers, Nat. Geosci., 5, 198-201, 2012.

Vignati, E., Karl, M., Krol, M., Wilson, J., Stier, P., and Cavalli, F.: Sources of uncertainties in modelling black carbon at the global scale, Atmos. Chem. Phys., 10, 2595-2611, 2010.

Wu, X., LI, Q., Wang, L., Pu, J., He, J., and Zhang, C.: Regional characteristics of ion concentration in glacial snowpits over the Tibetan Plateau and source analysis, Environment Science, 32, 971-975, 2011 (in Chinese with English abstract).

Xie, Z., Wang, X., Kang, E., Feng, Q., Li, Q., and Cheng, L.: Glacial runoff in China: an evaluation and prediction for the future 50 years, Journal of Glaciology and Geocryology, 28, 457-466, 2006.

Xu, B., Cao, J., Hansen, J., Yao, T., Joswia, D. R., Wang, N., Wu, G., Wang, M., Zhao, H., and Yang, W.: Black soot and the survival of Tibetan glaciers, PNAS, 106, 22114-22118, 2009.

Xu, J., Zhang, Q., Li, X., Ge, X., Xiao, C., Ren, J., and Qin, D.: Dissolved organic matter and inorganic ions in a central Himalayan glacier--insights into chemical composition and atmospheric sources, Environ Sci Technol, 47, 6181-6188, 2013.

Xu, J. Z., Zhang, Q., Wang, Z. B., Yu, G. M., Ge, X. L., and Qin, X.: Chemical composition and size distribution of summertime $PM_{2.5}$ at a high altitude remote location in the northeast of the Qinghai–Xizang (Tibet) Plateau: insights into aerosol sources and processing in free troposphere, Atmos. Chem. Phys., 15, 5069-5081, 2015.

Yao, T.: Recent glacial retreat in High Asia in China and its impact on water resource in Northwest China, Sci. China Ser. D, 47, 1065-1075, 2004a.

Yao, T.: Relationship between calcium and atmospheric dust recorded in Guliya ice core, Chin. Sci. Bull., 49, 706-710, 2004b.

Yao, T., Thompson, L., Yang, W., Yu, W., Gao, Y., Guo, X., Yang, X., Duan, K., Zhao, H., Xu, B., Pu, J., Lu, A., Xiang, Y., Kattel, D. B., and Joswiak, D.: Different glacier status with atmospheric circulations in Tibetan Plateau and surroundings, Nat. Clim. Change, doi: 10.1038/nclimate1580, 2012.

Zhang, Q., Huang, J., Wang, F., Mark, L., Xu, J., Armstrong, D., Li, C., Zhang, Y., and Kang, S.: Mercury distribution and deposition in glacier snow over western China, Environ. Sci. Technol., 46, 5404-5413, 2012a.

Zhang, Q., Kang, S., Gabrielli, P., Loewen, M., and Schwikowski, M.: Vanishing High Mountain Glacial Archives: Challenges and Perspectives, Environ Sci Technol, 49, 9499-9500, 2015.

Zhang, Y., Liu, S., Shangguan, D., Li, J., and Zhao, J.: Thinning and shrinkage of Laohugou No. 12 glacier in the Western Qilian Mountains, China, from 1957 to 2007, Journal of Mountain Science, 9, 343-350, 2012b.

Zhao, R., Lee, A. K. Y., Huang, L., Li, X., Yang, F., and Abbatt, J. P. D.: Photochemical processing of aqueous atmospheric brown carbon, Atmos. Chem. Phys. Discuss., 15, 2957-2996, 2015.

531 **Table 1**. Sampling information for snow, ice and proglacial streamwater in this study.

Sample type	Sampling time	Resolution※	Sampling site	Number (n)	Index
Snowpit	30th July, 2014	5 cm	4989 m	15	DOC, absorbance, ions
Snowpit	25th August, 2015	5 cm	5050 m	23	DOC, absorbance, ions
Surface fresh snow	4th August, 2014	100 m	4450-4900 m	18	DOC
Surface ice	6th August, 2014	100 m	4350-4900 m	20	DOC
Surface snow	16th July, 2015	50 m	4350-4850 m	11	DOC
Surface ice	15th August, 2015	50 m	4350-4850 m	11	DOC
Surface ice	25th August, 2015	50 m	4350-4600 m	6	DOC, absorbance
Subsurface ice	25th August, 2015	50 m	4350-4600 m	5	DOC, absorbance
Proglacial streamwater	29th-30th July, 2014	2h (day),4h (night)	4210 m	17	DOC
Proglacial streamwater	20th May-9th October, 2015	Every day	4210 m	184	DOC

532 ※ for snowpit it is vertical resolution, for surface ice and snow it is horizontal distance.

533

534

535 **Table 2**. Comparison of DOC concentrations in snow, ice and proglacial streamwater from the glacier in this study
536 and glaciers in other regions.

Sites	DOC concentration ($\mu g\ L^{-1}$)	Sample types	References
Laohugou glacier (LHG)	332 ± 132	Snowpit	This study
Tanggula glacier (TGL)	217 ± 143	Snowpit	Yan et al. (2015)
Mount Everest (EV)	153 ± 561	Snowpit	
Mendenhall Glacier, Alaska	190	snowpit	Stubbins et al. (2012)
Greenland ice sheet	401 - 57	Snowpit	Hagler et al. (2007)
Laohugou glacier (LHG)	229 ± 104	Surface snow	This study
Greenland ice sheet	111	Surface snow	Hagler et al. (2007)
Juneau Icefield, Southeast Alaska	100 - 300	Fresh snow/snowpits	Fellman et al. (2015)
Laohugou glacier (LHG)	426 ± 270	Surface ice	This study
Mount Nyainqentanglha Glacier	212	Glacier ice	Spencer et al. (2014)
Antarctic ice sheet	460 ± 120	Surface ice	Hood et al. (2015)
Alpine glacier	138 ± 96	Subsurface ice	Singer et al. (2012)
Laohugou glacier (LHG)	238 ± 96	Proglacial streamwater	This study
Mount Nyainqentanglha Glacier	262	Proglacial streamwater	Spencer et al. (2014)
Mendenhall Glacier, Alaska	380 ± 20	Proglacial streamwater	Stubbins et al. (2012)

537

538

539 **Table 3**. Mass absorption cross section (MAC) and Absorption Ångström Exponent ($AAE_{330-400}$) of ice and snow
540 from LHG glacier and aerosols from other regions.

Site/Source	MAC (m^2 g^{-1})	$AAE_{330-400}$	λ (MAC)	References
LHG glacier	1.4 ±0.4 (snow) 1.3 ±0.7 (ice)	5.0 ±5.9 (snow) 3.4 ±2.7 (ice)	365	This study
Biomass smoke	5.0	4.8	350	Kirchstetteret al. (2004)
Secondary organic aerosols	0.001 - 0.088	5.2 - 8.8	405	Lambe et al. (2013)
Wood smoke	0.13 - 1.1	8.6 - 17.8	400	Chen and Bond (2010)
HULIS, Arctic snow	2.6 ±1.1	6.1※	250	Voisin et al. (2012)
Beijing, China (winter)	1.79 ±0.24	7.5	365	Cheng et al. (2011)
Beijing, China (summer)	0.71 ±0.20	7.1	365	Cheng et al. (2011)

541 ※ the wavelength range for AAE of this study is 300 - 550 nm

542

543

Figure 1. Location map of LHG glacier No. 12.

Figure 2. Average DOC concentrations of ice, snow and proglacial streamwater for LHG glacier.

Figure 3. Variation in DOC concentrations in profiles of studied snowpits. The gray rectangles are dirty layers.

Figure 4. Exponential deceases in DOC concentrations during the biodegradation experiment. Note: The blue point is calculated using equations derived from the experimental data (black point).

Figure 5. Absorption spectra for DOC in snow and ice of LHG glacier and the dust from surrounding areas.

Figure 6. Comparison of DOC concentrations (A) and MAC_{365} (B) between surface and subsurface ice.

Figure 7. The discharge, DOC concentrations and fluxes exported from LHG glacier. Note: The concentrations with error bars include more than one sample on that day.

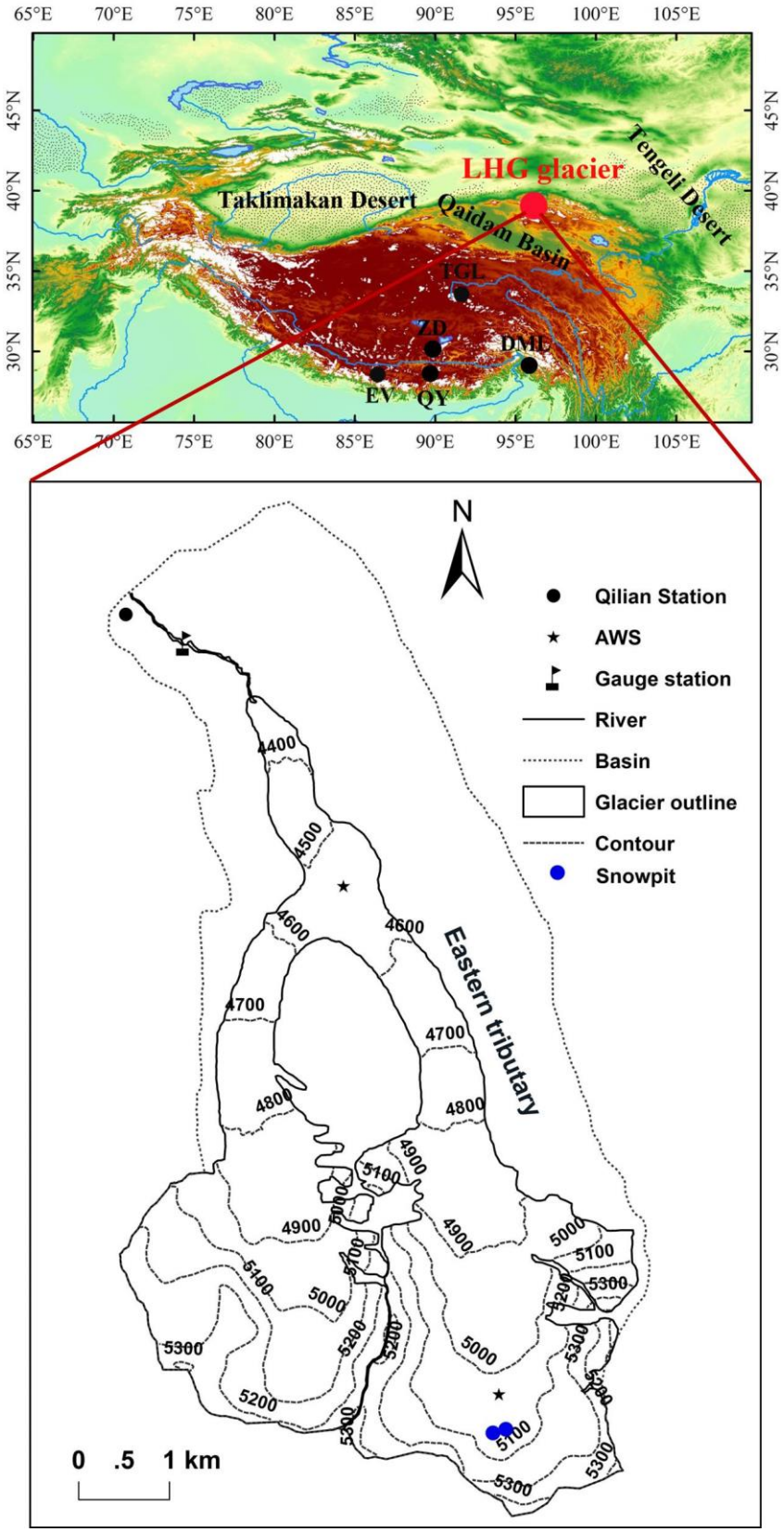

Figure 1. Location map of Laohugou glacier No. 12.

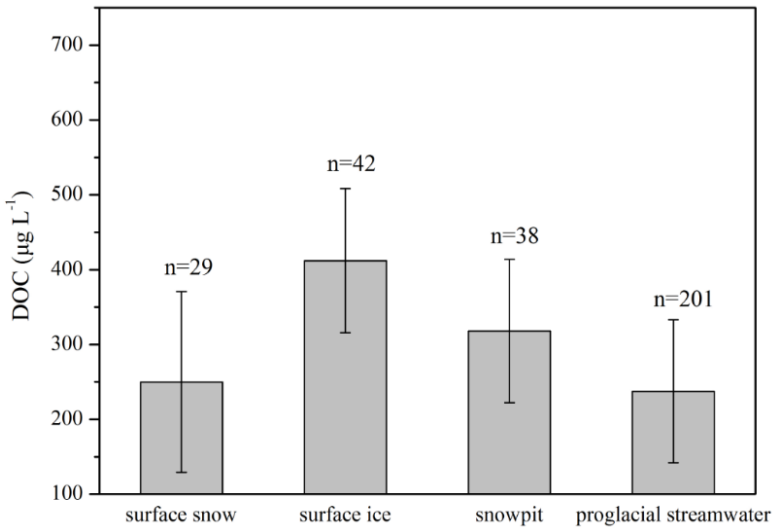

Figure 2. Average DOC concentrations of ice, snow and proglacial streamwater for LHG glacier.

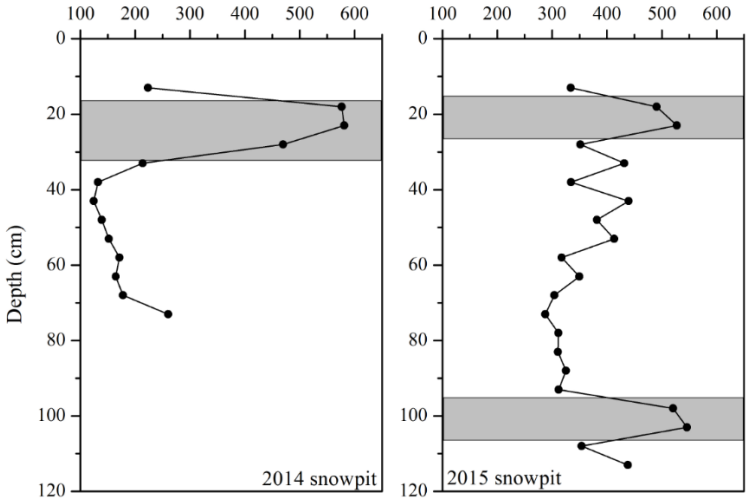

Figure 3. Variation in DOC concentrations in profiles of studied snowpits. The gray rectangles are dirty layers.

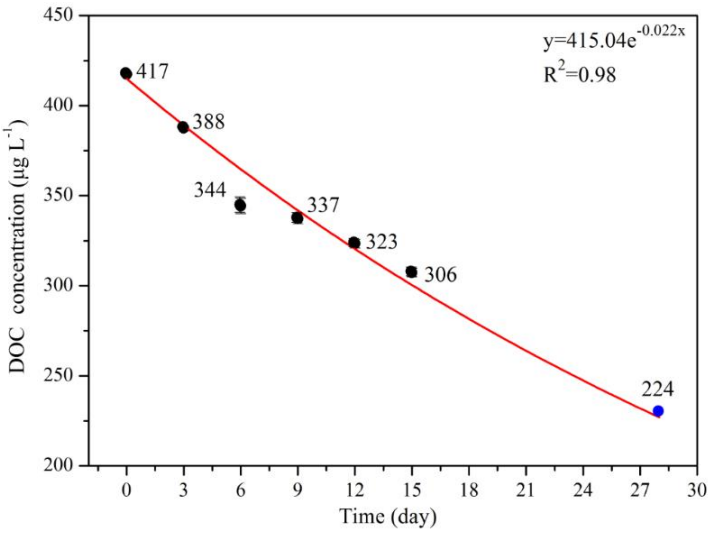

Figure 4. Exponential deceases in DOC concentrations during the biodegradation experiment. Note: The blue point is calculated using equations derived from the experimental data (black point). Mean values ± standard deviations of duplicate treated samples are presented.

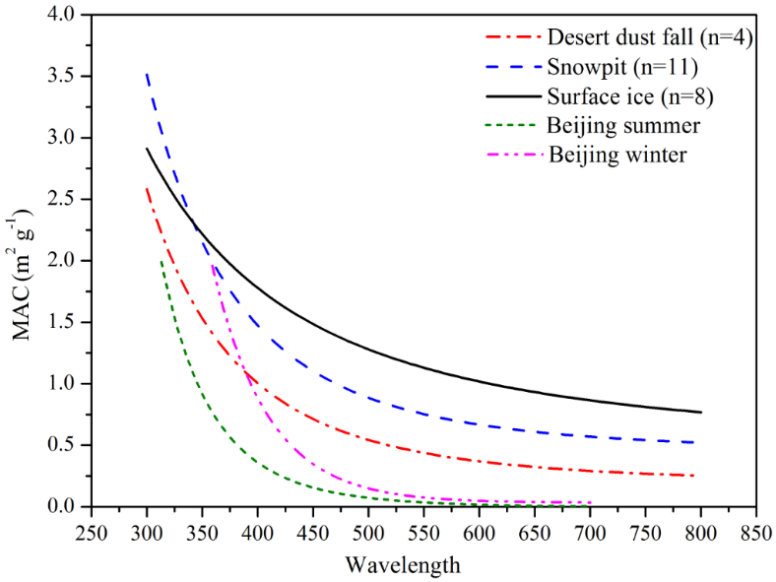

582

583 **Figure 5**. Absorption spectra for DOC in snow and ice of LHG glacier and the dust from surrounding areas.

584

585

586

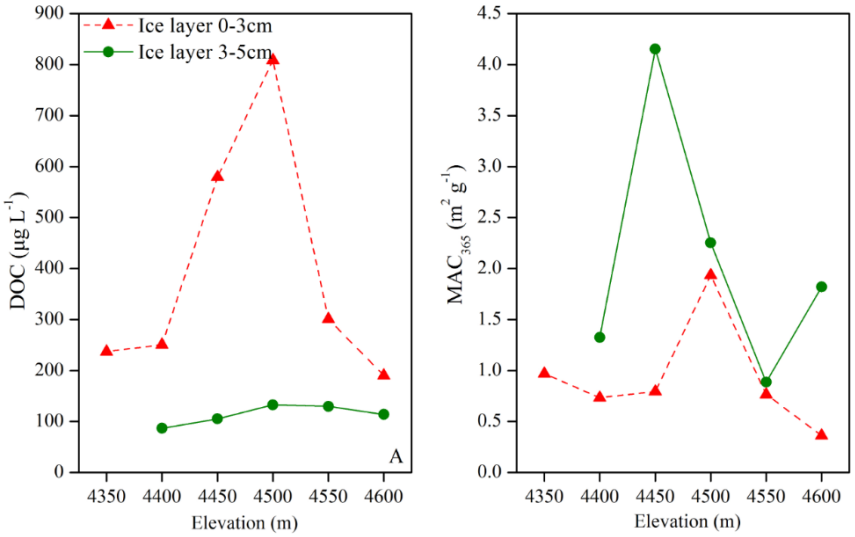

587

588 **Figure 6**. Comparison of DOC concentrations (A) and MAC_{365} (B) between surface and subsurface ice.

589

590

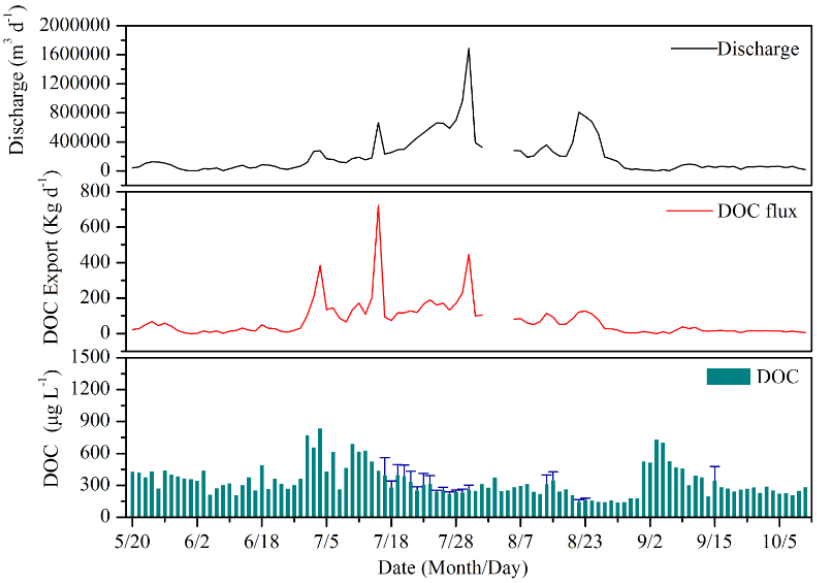

591

592 **Figure 7**. The discharge, DOC concentrations and fluxes exported from LHG glacier. Note: The concentrations
593 with error bars include more than one sample on that day.

594

595